

Linking biological variation to outcomes of statin treatment in the general population

Iryna Hlushchenko¹, Mohammad Majharul Islam¹, Max Tamlander², Samuli Ripatti^{2,3,4} and Simon G. Pfisterer¹

Affiliations:

- 1) Department of Anatomy, Faculty of Medicine, University of Helsinki, Finland
- 2) Institute for Molecular Medicine Finland, FIMM, HiLIFE, University of Helsinki, Helsinki, Finland
- 3) Clinicum, Department of Public Health, University of Helsinki, Helsinki, Finland
- 4) Broad Institute of MIT and Harvard, Cambridge, MA, USA.

Corresponding author: Simon Pfisterer (simon.pfisterer@helsinki.fi)

Abstract

Background and aims

Large interindividual variability in achieved low-density lipoprotein cholesterol (LDL-C) concentration is known for statin recipients. Systematic profiling of cellular lipid trafficking pathways was performed to elucidate how biological variation contributes to treatment outcomes of statin therapy.

Methods

Using a multiplexed imaging platform 26 readouts for cellular lipid trafficking were obtained from leukocyte subpopulations for each person, including LDL uptake (UPT), lipid storage (LiM) and three combined lipid trafficking scores (LT-P, LT-R, LT). With this pipeline 400 subjects of the FINRISK 2012 Study were analysed, including 200 recipients of cholesterol-lowering medication.

Results

Large interindividual variability of cellular LDL uptake and lipid storage was observed. Both LDL uptake and LT score associated negatively with LDL-C for statin recipients and the associations strengthened with increase in statin intensity, explaining up to 25% of LDL-C variability. Integration of LT score with a polygenic risk score for LDL-C further increased the association strength. High-intensity statin (HIS) recipients in the lowest quintile of LT score displayed a pro-atherogenic lipoprotein profile containing more VLDL, IDL and LDL particles with altered lipid content as compared to subjects in the highest quintile of the score. Subjects in the lowest quintile of the LT-R score had lower odds to be at their target LDL-C level and subjects in the lowest quintile of LiM score had higher odds to experience a cardiovascular event as compared to the rest of the HIS recipients.

Conclusions

Interindividual variation in cellular lipid trafficking pathways can contribute to the variability of statin therapy outcomes and provide new opportunities for treatment optimization and risk assessment in cardiovascular disease.

NOTE: This preprint reports new research that has not been certified by peer review and should not be used to guide clinical practice.

Keywords: LDL-cholesterol, LDL uptake, biological variation, lipid storage, lipid droplet, statin medication, polygenic risk score

Translational perspective

Most high-risk patients do not achieve their LDL-C target levels and have limited access to lipid-lowering treatment (LLT) beyond statins. Here we highlight that cellular readouts for lipid uptake and storage can be used to understand why statin therapy benefits some patients more than others. This can open new avenues for precision medicine applications for easier selection of optimal LLT and improved cardiovascular risk assessment.

Introduction

Hypercholesterolemia is a global health problem and the leading cause of cardiovascular disease (CVD).¹ Even though multiple treatment options exist, such as statins, ezetimibe or PCSK9 inhibitors, a large fraction of high-risk patients does not achieve desired low-density lipoprotein cholesterol (LDL-C) levels.²⁻⁴ The reasons for poor goal attainment are multifactorial, including low adherence, as well as challenges imposed through healthcare systems and reimbursement rules.⁵⁻⁸ On the other hand, it is plausible that biological variation in the cellular pathways underlying drug action represents an important contributing factor to goal attainment, but lacks experimental data to receive recognition.

Statins and PCSK9 inhibitors (PCSK9i) influence cellular lipid trafficking via different mechanisms. Whilst PCSK9i block degradation of the low-density lipoprotein (LDL) receptor (LDLR), statins evoke cellular cholesterol depletion and increased LDLR expression.⁹⁻¹¹ In both cases more abundant plasma membrane LDLR results in increased LDL uptake and clearance from the blood. Cell surface abundance of LDLR is linked to cellular lipid homeostasis, with excess cholesterol and lipid storage resulting in reduced LDLR expression.^{12,13}

For familial hypercholesterolemia (FH) patients, alterations in cellular LDL uptake have been linked to treatment outcomes for statin¹⁴⁻¹⁷ and PCSK9i medication.¹⁸ Initially, cellular LDL uptake studies were designed to identify FH patients.¹⁹ However, differentiation of FH patients from control individuals was difficult, due to interindividual variability in both groups.²⁰ Previously, we have established a multiplexed automated analysis pipeline for systematic quantification of cellular LDL uptake and lipid storage in leukocyte subpopulations under different cholesterol depletion states, providing 26 readouts on lipid trafficking for each subject.¹⁴ We demonstrated that monocytes display more robust responses

in both LDL-uptake and lipid storage than lymphocytes and that individuals with identical LDLR mutations display highly divergent LDL uptake profiles which are associated with achieved LDL-C on statin therapy.¹⁴ This highlights that variations in cellular lipid trafficking pathways are likely widespread, however, it is yet unclear whether they are relevant for lipid-lowering treatment outcomes and cardiovascular disease progression in the general population.

The main objective of this study was to elucidate how LDL-uptake and lipid storage in leukocyte subpopulations associate with circulating LDL-C and different lipoprotein subclasses in statin users from the general population cohort, versus subjects not on lipid-lowering therapy. Secondary goals were to examine if poor lipid trafficking profiles are associated with increased cardiovascular risk and to investigate the interrelationship of cellular and genetic risk scores.

Methods

Study design and group definitions

We selected 200 recipients of lipid-lowering therapy and 200 matched controls from the FINRISK 2012 population survey for whom frozen PBMC samples were stored in THL Biobank. These two subject groups were defined based on questionnaire answers and were matched by age, sex, BMI and use of blood pressure medication. We obtained laboratory lipid values (Total cholesterol, LDL-C, triglycerides, APO-B, APO-A1), age, sex and BMI for all of the selected individuals. NMR metabolomics values were available for 398 subjects and polygenic risk scores could be calculated for 394 participants. For optimal performance of the cellular assays 1.6 million viable cells are required per each subject. We could obtain only one of two tubes of cryopreserved PBMCs stored in the Biobank for each subject. The amount of viable cells per subject ranged from zero to 5.5 million, therefore we could obtain reliable cellular readout results from 273 samples (135 controls and 138 cases).

For a precise definition of the used lipid-lowering medication we utilised drug purchase history for 2002-2019 obtained from the Finnish Social and Health Data Permit Authority Findata. We selected subjects who purchased lipid-lowering medication during 6 months prior to sampling. The last two purchases before sampling defined the medication type. This strategy resulted in selection of 202 subjects of whom 191 were on statin monotherapy (simvastatin n=127, atorvastatin n=30, rosuvastatin n=22, fluvastatin n=3, lovastatin n=3, pravastatin n=6). Since 94% of subjects were on either simvastatin, rosuvastatin or atorvastatin therapy we included only these three statin types in the further subgroup formation. We further extracted the purchased statin doses from the records and defined statin intensity groups based on previously reported LDL-c reductions from baseline achieved with different doses of simvastatin, rosuvastatin and atorvastatin: >35% LDL-c

reduction from the baseline (rosuvastatin 5-40 mg, atorvastatin 10-80 mg, simvastatin 40-80 mg), >40% (rosuvastatin 5-40 mg, atorvastatin 10-80 mg) and >45% (rosuvastatin 10-40mg, atorvastatin 20-80 mg).²¹⁻²³

We have conducted the initial association analyses for the subjects for whom both cellular data and NMR metabolomics values were available. Before integration of cellular score with LDL-PRS, subjects missing the latter were removed (Supplementary Figure 1).

Definition of CVD events for risk assessment

Cardiovascular disease events were defined as myocardial infarction or ischemic stroke specified by I2X and I6X diagnosis codes from the International Statistical Classification of Diseases and Related Health Problems 10th Revision (Supplementary Methods). Both prevalent and incident CVD events were included and were extracted from hospital admission and primary care electronic health records.

Human subject samples

Peripheral blood mononuclear cell (PBMC) samples were cryopreserved in 2012 as a part of Finnish population survey, FINRISK 2012, with written consent and ethical approval of the Hospital District of Helsinki and Uusimaa (permit 162/13/03/00/2011).²⁴ The FINRISK 2012 sample collection was then transferred to THL Biobank in 2015. Frozen PBMC samples, pseudonymised donor-linked lipid values and survey data were obtained then from THL Biobank (www.thl.fi/biobank) and used under Biobank agreement (THLBB2020_7). A mixture of PBMCs from four healthy donors were used as standards for assay measurements. These cells were isolated by density-gradient centrifugation from buffy coat samples obtained through the Finnish Red Cross Blood Service (56/2019).

PBMC recovery

Cryopreserved samples were thawed and cell viability was determined using trypan blue exclusion technique. Cells were then seeded into 96-well plates for 24-hour incubation with lipid-rich (R) medium (RPMI-1640 supplemented with 2mM L-Glutamine, 100 units/mL potassium penicillin, 100ug/mL streptomycin sulphate, 5mM HEPES and 1mM sodium pyruvate) containing 10% foetal bovine serum or lipid-poor (P) medium containing 5% lipoprotein-deprived serum. The cellular assays were performed in 384-well plate format on the next day.

LDL uptake and lipid droplet assays

Fluorescent labelling of low-density lipoprotein particles with DiI²⁵⁻²⁷, LDL uptake and lipid droplet assays¹⁴ were described previously. DiI-LDL was spiked into the growth media to achieve a final concentration of 30 µg/mL and the cells were further incubated for 1 hour at 37°C. Subsequently, the cells were washed and resuspended with serum-free growth medium. Next, using an open-source robotic platform (Opentrons, New York, USA) the cells were transferred and adhered to coated 384-well imaging plates. Afterwards, cells were automatically fixed with 4% PFA, washed and stained with nuclear marker DAPI (5 µg/ml) and cytoplasm marker CellMask™ DeepRed (0.5 µg/ml). For lipid droplet analysis the cells were fixed and stained in the same manner as in the LDL uptake assay except that the staining solution contained 5 µg/ml DAPI and 1µg/ml LD540 (Princeton BioMolecular Research).²⁸ Images were acquired for both assays with a PerkinElmer OperaPhenix automated spinning disc confocal microscope using a 40x or 63x water immersion objective. Each assay was repeated twice and two PBMC standard samples were included in every experiment. Each analysis batch included matched cases and controls.

Image processing and quantification

Raw confocal 3D image stacks were automatically deconvolved and collapsed into the maximum intensity projections using a custom-made Python tool (<https://github.com/lopaavol/OPutils>). Then cell nuclei, cytoplasm and organelles were segmented automatically using CellProfiler.²⁹ Several images from each plate were sampled and inspected by the experimenter for potential segmentation errors to ensure segmentation quality and to filter out imaging artefacts.

Genotyping, imputation and LDL-c polygenic risk score (LDL-PRS)

We obtained genotypes for 394 of our 400 study individuals from THL Biobank for which single nucleotide polymorphism (SNP) array and centrally imputed genotype data were available. The FINRISK 2012 samples were genotyped using the Illumina HumanCoreExome-24 v1.1 and Affymetrix Axiom FinnGen1.r1 and FinnGen1.r2 arrays. The genotype imputation workflow with pre- and post-imputation quality control steps was carried out as described in the following protocol: [dx.doi.org/10.17504/protocols.io.xbgfijw](https://doi.org/10.17504/protocols.io.xbgfijw).

We used PLINK 2.0³⁰ to first convert PED and MAP files obtained from THL Biobank to BED, BIM and FAM files, and then calculated a genome-wide LDL-PRS using weights for a LDL-PRS calculated in FinnGen³¹ study Data Freeze 7 (available at: <https://www.pgscatalog.org/score/PGS002764/>). Our final LDL-PRS included 1,086,403 variants and could be calculated to 394 out of 400 subjects. Next, we normalised LDL-PRSs to zero to one range. Contrary to cellular scores, LDL-PRS was positively associated with LDL-c levels in our study (Supplementary Figure 2) and in previously reported FINRISK 2012 cohort analysis.³² Therefore, to allow for comparability of LDL-PRS to cellular lipid trafficking scores and their further integration we inverted LDL-PRS for all the downstream analyses.

Subject health data retrieval

General information about subjects' age, sex, weight, BMI, waist and hip circumference, lifestyle and medication status (lipid-lowering, diabetes and blood pressure) as well as standard laboratory lipid values and NMR metabolomics values were retrieved in conjunction with samples from THL Biobank. Additionally the pseudonymised medical records related to cardiometabolic disorders for each patient were obtained for years 2002–2019 from Finnish primary care register (Avohilmo) and national social and healthcare data collection and reporting system (Hilmo). Records of purchase and reimbursement of lipid-lowering medications for years 2002–2019 were obtained from the Social Insurance Institution of Finland (Kela). All data extraction procedures were done under permit (THL/4640/14.02.00/2020) and handled by Findata.

Data processing and statistical analysis

Data was processed using Python standard libraries (Python Software Foundation, www.python.org) and the following packages: Pandas,³³ Numpy,³⁴ Scipy,³⁵ Matplotlib,³⁶ Scikit-Learn,³⁷ Seaborn³⁸. Single-cell readouts were filtered for cell size and mean intensity outliers with 5 SD from mean being the cut-off point. On average several hundred monocytes and several thousand lymphocytes were quantified in each well. Wells with less than 50 cells were discarded from the analysis. We further obtained mean per-well values for intensity and organelle numbers. For each of lipid-rich (R) and lipid-poor (P) conditions we analysed four wells in two independent experiments. Absolute values were then normalised to the included control samples. LDL uptake and lipid mobilisation for the entire dataset were additionally rescaled to zero to one range before combining into lipid trafficking scores.

Statistical analyses were performed with python package `scipy.stats`. For pairwise comparisons of group means reported in Table 1 the Student's T-test was used. To determine

the correlations between cellular scores and lipid values the Spearman rank-order correlation coefficients and corresponding asymptotic P values were calculated. To test the difference between lipid species concentrations in controls versus subgroups of statin recipients (Figure 3D) we used Mann-Whitney U test. Odds ratios were calculated using 2x2 contingency tables and corresponding P values were calculated using Fisher's exact test. The 95% confidence intervals (CI) were calculated using the standard formula for CI for odds ratios. Due to small sample size in some cases the contingency tables contained zero values and therefore produced zero or infinite odds ratios, to calculate an estimated odds ratio in these cases a value of 0.5 was added to each value in a 2x2 table.

Results

Turning multiparametric readouts into cellular lipid trafficking scores

Peripheral blood mononuclear cell (PBMC) samples were analysed with an automated pipeline for detailed quantification of LDL uptake and lipid storage as described previously.¹⁴ In the LDL-uptake assay we quantified the mean intensity of internalised fluorescently labelled LDL (Int) and the number of LDL-filled organelles (No) in lymphocyte and monocyte populations under lipid-rich and -poor conditions (Figure 1A, C). Mean intensities and organelle counts were normalised to controls and combined for each condition into an uptake score for lipid-rich (UPT-R) and lipid-poor conditions (UPT-P) (Figure 1C).

In the lipid storage assay we analysed lipid droplets in lipid-rich and -poor conditions, quantifying the number of lipid droplets (LD-No) and the total lipid droplet area (LD-Area) in every lymphocyte and monocyte as well as the percentage of lipid droplet-positive cells (LD-Pos) for lymphocyte and monocyte populations (Figure 1B). Both lymphocytes and monocytes tended to deplete the lipids stored in lipid droplets when challenged with lipid-poor conditions. We expressed this by dividing the values of lipid droplet parameters in lipid-rich and -poor conditions and further combining these three values into a single lipid mobilisation score (Figure 1C). Moreover, we combined lipid mobilisation and LDL uptake scores into composite lipid trafficking scores for lipid-rich (LT-R) and -poor (LT-P) conditions, and into a single lipid trafficking (LT) score with all readouts combined (Figure 1C). This enabled us to look at individual cellular parameters as well as their combinations when integrating the data with physiological and clinical outcomes.

Subject group characteristics

All the relevant cellular readouts and NMR metabolomics data were available for 135 control subjects and 133 recipients of statin monotherapy. We divided the group of statin recipients into sub-groups with increasing statin intensity based on reported LDL-c

reductions from baseline achieved on different doses of simvastatin, atorvastatin and rosuvastatin.²¹⁻²³ Of the subjects with available cellular readouts only 60 received a statin dose enabling at least a 35% reduction in LDL-C from baseline (>35% group), 39 participants received therapy with a potential to reduce LDL-c by at least 40% (>40% group) and 30 people with the potential to reduce LDL-C by more than 45% (>45% group). We are referring to both >40% and >45% groups as recipients of high-intensity statin (HIS) medication (Supplementary Figure 1).

The percentage of males in the formed groups was 44% to 55% (Table 1). We observed small differences in BMI for statin users of the >45% group (29.7 vs 27.8 in controls) (Table 1). As expected, subjects receiving statins had lower total cholesterol (4.61 mmol/L, statin vs. 5.65, controls) and LDL-c levels (2.51 mmol/L, statin vs. 3.48, controls) (Table 1).

Association of lipid trafficking scores with LDL-cholesterol, APO-B and total cholesterol.

Next, we investigated whether cellular readouts on lipid trafficking are associated with circulating lipid markers such as LDL-C, total cholesterol and apolipoprotein(B) (APO-B) for the different subject groups. Similar to our previous observations from FH patients, monocyte LDL uptake parameters showed a negative correlation with plasma LDL-C for statin recipients (Figure 2A and Supplementary Figure 3A,B).¹⁴ This correlation was more pronounced for the quantification of LDL-filled organelles (LDL-No) (Figure 2A) as compared to cellular LDL intensity (LDL-Int) (Supplementary Figure 3A) when measured in lipid-poor condition. Stronger associations were also seen in measurements in lipid-poor conditions as compared to lipid-rich conditions (Figure 2A, Supplementary Figure 3B) and when quantified in monocytes (Figure 2A, Supplementary Figure 3A) as compared to lymphocytes (Supplementary Figure 3C). The correlation strength for both LDL-No and

LDL-Int with LDL-C increased when shifting towards higher statin intensity, except for the '>45%' group. Similar correlations were obtained for total cholesterol and APO-B (Figure 2C). For the '>40%' statin group, LDL-No explained 16% of the variability of the circulating LDL-C (coefficient of determination $R^2=0.16$, $p=0.01$), 14% of the total cholesterol ($R^2=0.14$, $p=0.02$) and 13% of APO-B ($R^2=0.13$, $p=0.02$).

The lipid mobilisation score provided weak associations with LDL-C across the different groups and only saw an increase in the '>45%' group (Supplementary Figure 3D). Combination of the lipid uptake scores with the lipid mobilisation score into the lipid trafficking (LT) score (Figure 1C) provided stronger associations with LDL-C than LDL-No, with consistent increases for each statin intensity group (Figure 2A) and explaining 25% of the variability of LDL-C for the '>45%' group ($R^2=0.25$, $p=0.005$).

Overall, LDL-No and the LT score from monocytes associated with LDL-C, total cholesterol and APO-B, with increasing strength for higher statin intensity. The LT score provided more robust results across the different subject groups, including the smallest '>45%' statin group.

Lipid trafficking scores associate with a pro-atherogenic lipoprotein profile

To investigate whether alterations of cellular lipid trafficking impacts also other lipid particles and species, we extended our study with NMR metabolomics, providing access to 213 biomarkers, including concentration and composition of 14 lipoprotein particle classes.

Based on our observations with LDL-C we utilised the LT score for correlations with the NMR metabolomics data. For control subjects, LT score showed a weak negative association with cholesterol ester and triglyceride concentration in large HDL particle fractions (Figure 3A) and with sphingomyelin (Figure 3C). When focusing on the statin group with an LDL-C-lowering potential of more than 40%, LT score correlated negatively with XS-VLDL, IDL, L-LDL, M-LDL, and S-LDL particle concentrations (Figure 3B).

Higher cholesterol ester concentrations, in particles from S-VLDL to S-LDL were observed for subjects from the '>40%' group with a low LT score, whilst associations with triglycerides were less pronounced (Figure 3B). Correlations with the % lipid distribution across lipid particles were changed compared to controls. '>40%' -subjects with low LT score displayed a higher share of cholesterol ester in small VLDL, IDL and LDL particles, whilst in large and medium sized HDL particles the share dropped (Figure 3B). Vice-versa, % triglycerides were lower in small VLDL and IDL particles for subjects with low LT score from the '>40%' group (Figure 3B).

Besides cholesterol esters, a low LT score also negatively correlated with increased sphingomyelin for the '>40%' group (Figure 3C). Other lipid species were also increased for subjects with low LT, but association was less profound as compared to sphingomyelin.

Whilst '>40%' subjects within the highest quintile of the LT score achieved substantial reductions in cholesterol ester concentrations of S-, XS-VLDL, IDL and LDL particles (Figure 3D), those within the lowest quintile did not and displayed cholesterol ester concentrations equivalent to subjects without cholesterol-lowering medication (Figure 3D).

Taken together, our NMR metabolic data highlights that individuals with impaired cellular lipid trafficking score display a pro-atherogenic lipoprotein profile on HIS therapy.

Lipid trafficking scores integrated with polygenic risk scores

Previously, we showed that cellular lipid trafficking scores did not associate with a polygenic risk score for LDL (LDL-PRS) for individuals without cholesterol-lowering medication.¹⁴ Here we confirm this observation with a larger set of individuals (Figure 4A). On the other hand, the combined LDL uptake score in lipid-poor conditions (UPT-P) correlated with LDL-PRS for subjects of the '>40%' group, whilst the lipid mobilisation score and lipid trafficking score did not (Figure 4A). LDL-PRS correlated with LDL-C for statin users and, interestingly, the association strength increased within higher statin intensity

groups (Figure 4B), except for the '>45%' group, similar to the cellular LDL-No scores (Figure 2A). Based on these results we evaluated whether combination of LT score with LDL-PRS would lead to a higher association with LDL-C as compared to the individual scores alone. The combined score showed significant associations with LDL-C for all statin groups and also control individuals (Figure 4B). For the '>45%' group the combined score explained 29.7% of the LDL-C variability ($R^2=0.297$, $p=0.002$), a 5.1% increase over the LT score (Figure 2A) and 20.6% over the LDL-PRS ($R^2=0.09$, $p=0.1$). Then, we extended this analysis to the NMR metabolomic data (Figure 4C). Similar to the lipid trafficking score, a poor LDL-PRS associated with pro-atherogenic lipoprotein particles, with higher cholesterol ester and triglyceride content for subjects of the '>40%' group (Figure 4C). Even though the % distribution of cholesterol esters and triglycerides was more affected by the LT score (Figure 4C, Figure 3B) combination of the LDL-PRS with the lipid trafficking score further improved the association strength with the pro-atherogenic lipoprotein profile (Figure 4D), explaining, for example, up to 37.7% of the variability ($R^2=0.377$, $p<0.001$) of cholesterol ester concentration in XS-VLDL particles of '>40%' subjects.

Lipid trafficking scores enable stratification for LDL target level attainment

Next, we investigated whether lipid trafficking scores and LDL-PRS could enable the definition of subject sub-groups who are at higher or lower odds to achieve their LDL-C treatment goals. According to the 2011 ESC/EAS guidelines³⁹ that were in use during the sample collection, LDL-C goal of <1.8 mmol/l was recommended for very high CV risk and a goal of <2.5 mmol/l for high CV risk patients. We adopted these recommendations for our goal-attainment analysis defining subjects with a history of myocardial infarction or stroke as being at very high risk and subjects without such a history at high risk. Subjects in each group were then divided into quintiles for the different LT scores and we evaluated whether subjects within the highest or lowest quintile achieved LDL-C target levels. Whilst all LT scores

showed the same tendency, LT-R (a combination of LDL uptake scores quantified from monocytes in lipid-rich conditions with the lipid mobilisation score) was the best at stratifying subjects for reaching their LDL target levels. We then looked at the performance of the LT-R, LDL-PRS and a combined LDL-PRS/LT-R score (Figure 5).

Those subjects within the highest LT-R quintile displayed better goal attainment than unstratified subjects across the different study groups and goal attainment further increased in high-intensity statin groups (Figure 5A). For both '>40%' and '>45%' groups all subjects within the highest LT-R quintile achieved their LDL target goals, therefore we used estimates of the odds ratios for these subgroups (Figure 5 A,B). Looking at those subjects within the highest LDL-PRS quintile only provided marginal improvements for goal attainment above unstratified subjects of the control group (Figure 5A,B). Also, combining LT-R and LDL-PRS did not provide added value for subjects on statin medication. However, for those without statin medication, combining LT-R and LDL-PRS enabled the definition of a subject subgroup with a five-fold higher odds to achieve target LDL-C levels (OR=5.2, 95% CI [1.74, 15.6]) compared to the rest of the group (Figure 5B).

Without statin medication, none of the subjects within the lowest LT-R quintile achieved LDL-C target levels (Figure 5C, D). Goal attainment increased for subjects of the same LT-R quintile when looking at the entire statin group, but then dropped for subjects in groups with higher statin intensity. In the '>40%' group, only 12.5% of subjects within the lowest LT-R quintile achieved their LDL-C goal and no subjects within the lowest quintile achieved their goal in the '>45%' group (estimated OR=0.02, 95% CI [0.001, 0.475] $P<0.001$). Also individuals within the lowest LDL-PRS quintile were at lower odds to achieve their LDL-C targets (Figure 5C,D), but LT-R showed stronger effects. Combination of LDL-PRS and LT-R improved the definition of subjects who did not achieve LDL-C target levels, especially in the '>35%' and '>40%' statin groups.

Lipid trafficking scores in risk assessment of cardiovascular disease

During a seven-year follow-up of the 265 subjects, eleven (four in controls and seven in statin group) were diagnosed with myocardial infarction (MI) and ten with stroke (five in each of the two groups), resulting in 21 cardiovascular events. This allowed us to get a first impression whether cellular scores could aid in cardiovascular risk assessment.

Control subjects within the lowest quintile of lipid mobilisation score were at higher odds to experience a cardiovascular event as compared to the rest of the group with increasing effect size with the increase in statin intensity (Figure 6). There was a significant difference in the odds to experience a CV event between the lowest quintile of lipid mobilisation score and the rest of the subjects in both the '>40%' group and the '>45%' group (Figure 6). Combination of the lipid mobilisation score with the LDL uptake score from lipid-poor conditions increased the odds ratio of experiencing a cardiovascular event to 30 (95%CI [2.65, 339.75], p=0.004) for subjects in the lowest quintile of the '>40%' group, as compared to the rest of the group.

Discussion

Here, we performed the first systematic functional profiling of cellular lipid trafficking pathways for a set of subjects from the general population, observing extensive interindividual variability and widespread defects in cellular LDL uptake and lipid storage in leukocyte subpopulations. For subjects receiving high-intensity statin (HIS) medication, lower cellular LDL uptake and lipid trafficking scores were associated with increased LDL-C, IDL, small VLDL particles and a higher cholesterol ester content across APO-B containing lipid particle subclasses. Elevated LDL-C is responsible for the formation of atherosclerotic plaques and progression of cardiovascular disease.¹ Besides LDL, small VLDL and IDL can cross the endothelial cell barrier and remnant cholesterol is a known driver of atherosclerosis.^{40,41} We further observed elevated sphingomyelin concentrations for subjects with a poor lipid trafficking score. A higher amount of sphingomyelin in LDL particles renders them more prone to aggregation and stimulates atherosclerosis.⁴² Consequently, HIS recipients with a low lipid trafficking score display several pro-atherogenic modifications to their lipoprotein profile. Finally, our data show that HIS recipients with a poor lipid mobilisation or lipid trafficking score are at increased risk for cardiovascular disease.

Our observations are supported by genetic studies which link loss-of-function variants of the LDLR receptor to a higher incidence of cardiovascular disease.^{43,44} Whilst the detection of an LDLR loss-of-function variant implies a defective LDL uptake response, we directly quantify this cellular process with high-content microscopy of leukocyte cell populations. It is known that individuals from the general population can have a cellular LDL uptake potential which is similar to heterozygous familial hypercholesterolemia patients with loss-of-function LDLR mutations.²⁰ Our study supports these findings, and highlights for the first time the physiological and clinical consequences for subjects with lipid trafficking

defects equivalent to the FH phenotype. Alterations of the lipid profile and increased cardiovascular risk are more profound when subjects with a poor lipid trafficking score are receiving HIS medication. This may reflect an increased reliance on cellular LDL uptake pathways when cholesterol synthesis is blocked in statin recipients. In support, statin intake elevates the expression of liver LDL receptors.^{9,45} In such a scenario, subjects with a reduced LT score may have a limited ability to efficiently clear pro-atherogenic lipoproteins upon statin therapy.

Similar to the lipid trafficking score, association strength of LDL-PRS with LDL-C increased with higher statin intensity. A potential explanation for this could be that a portion of the single nucleotide polymorphisms contained in the LDL-PRS is linked to cellular LDL uptake. Our observation that cellular LDL uptake correlates with the LDL-PRS for HIS recipients supports this hypothesis. Apparently, LDL-PRS and lipid trafficking scores have non-overlapping features as well, which would explain why a combination of the LDL-PRS with the lipid trafficking score provided a better association with pro-atherogenic lipoprotein particles and in some instances improved patient stratification for goal attainment.

Recent studies highlight difficulties in goal attainment for patients on statin medication and in making the switch to combination therapy.² Systematic quantification of cellular lipid trafficking pathways may aid in the identification of patients who are refractory to statin medication, remain at increased cardiovascular risk and are in need of additional medication. This is supported by our observation that individuals with a poor lipid trafficking score do not achieve their LDL-C goals on HIS medication. In our study all subjects with a good lipid trafficking score achieved their LDL-C goals on HIS therapy, a piece of information which may be important for physicians as well. Consequently, systematic functional profiling may provide relevant insight into the variability of cellular mechanisms underlying drug action and disease progression, making risk assessment and treatment

selection easier, a diagnostic cellular test could provide insight into cellular disease mechanisms.

Strengths

We acquired a comprehensive set of functional cell data for 273 individuals from the FINRISK 2012 population survey. The analysis strategy is based on a semi-automated workflow with fully automated microscopy and image analysis. This reduces researcher bias and increases the reproducibility of our results. Our focus on automation makes it possible to scale the analysis to higher throughput, enabling clinical applications in the future.

Limitations

Our observations for HIS recipients are derived from a limited number of subjects from the Finnish population survey FINRISK 2012. This might limit the applicability of our observations to other populations, especially those with different ethnic backgrounds. Furthermore, patient stratification for goal attainment and risk assessment is limited to persons who were on statin monotherapy at sampling time. Readers should also keep in mind that the medication status of the subjects in this study was determined by their drug purchase patterns. Whilst this method gives a more detailed picture compared to the yes/no type of questionnaire initially available, it can not verify if the subjects were in practice adherent to the therapy.

Conclusions

Overall this study highlights that intraindividual variation of biological processes should receive more attention in the treatment of hypercholesterolemia, enabling patient stratification for better treatment and improved risk assessment of cardiovascular disease.

Acknowledgements

The samples and sample-related data used for the research were obtained from THL Biobank (study number: THLBB2020_7). We thank all study participants for their generous participation at THL Biobank and FINRISK 2012 Study.

Funding

Grants from the Academy of Finland 328861 and 325040, Business Finland (Research to Business) 1821/31/2021, Magnus Ehrnrooth and the Foundation for Cardiovascular Research to S.G.P. Grants from Academy of Finland Center of Excellence in Complex Disease Genetics 312062, Academy of Finland 285380, the Finnish Foundation for Cardiovascular Research and the Sigrid Jusélius Foundation to S.R. Funding from the Doctoral Programme in Population Health, University of Helsinki to M.T.

Conflict of interest

A patent application covering the use of the here-suggested patient stratification methods has been filed (application: WO2022123120A1), in which University of Helsinki is the applicant and S.G.P. is an inventor.

Data availability statement

The data underlying this article were provided by THL Biobank (www.thl.fi/biobank) and used under Biobank agreement THLBB2020_7. Access to the data can be obtained from the THL Biobank through the standard application procedure. The register-based data used in this study can be obtained from the Finnish Social and Health Data Permit Authority Findata by submitting a data permit application. Description of the register data (names of registers and attribute codes) can be obtained from the corresponding author.

References

1. Borén J, Chapman MJ, Krauss RM, Packard CJ, Bentzon JF, Binder CJ, et al. Low-density lipoproteins cause atherosclerotic cardiovascular disease: pathophysiological, genetic, and therapeutic insights: a consensus statement from the European Atherosclerosis Society Consensus Panel. *Eur Heart J* 2020;**41**:2313–2330. doi: <https://doi.org/10.1093/eurheartj/ehz962>
2. Ray KK, Molemans B, Schoonen WM, Giovas P, Bray S, Kiru G, et al. EU-Wide Cross-Sectional Observational Study of Lipid-Modifying Therapy Use in Secondary and Primary Care: the DA VINCI study. *Eur J Prev Cardiol* 2021;**28**:1279–1289. doi: <https://doi.org/10.1093/eurjpc/zwaa047>
3. Ridker PM, Mora S, Rose L, JUPITER Trial Study Group. Percent reduction in LDL cholesterol following high-intensity statin therapy: potential implications for guidelines and for the prescription of emerging lipid-lowering agents. *Eur Heart J* 2016;**37**:1373–1379. doi: <https://doi.org/10.1093/eurheartj/ehw046>
4. Ballantyne CM. Achieving greater reductions in cardiovascular risk: lessons from statin therapy on risk measures and risk reduction. *Am Heart J* 2004;**148**:S3–S8. doi: <https://doi.org/10.1016/j.ahj.2004.04.025>
5. Katzmann JL, Kieble M, Enners S, Böhm M, Mahfoud F, Laufs U, et al. Trends in Ezetimibe Prescriptions as Monotherapy or Fixed-Dose Combination in Germany 2012–2021. *Front Cardiovasc Med* 2022;**9**:912785. doi: <https://doi.org/10.3389/fcvm.2022.912785>
6. Cohen JD, Cziraky MJ, Jacobson TA, Maki KC, Karalis DG. Barriers to PCSK9 inhibitor prescriptions for patients with high cardiovascular risk: Results of a healthcare provider survey conducted by the National Lipid Association. *J Clin Lipidol* 2017;**11**:891–900. doi: <https://doi.org/10.1016/j.jacl.2017.04.120>
7. Hirsh BJ, Smilowitz NR, Rosenson RS, Fuster V, Sperling LS. Utilization of and Adherence to Guideline-Recommended Lipid-Lowering Therapy After Acute Coronary Syndrome: Opportunities for Improvement. *J Am Coll Cardiol* 2015;**66**:184–192. doi: <https://doi.org/10.1016/j.jacc.2015.05.030>
8. Rodriguez F, Maron DJ, Knowles JW, Virani SS, Lin S, Heidenreich PA. Association of Statin Adherence With Mortality in Patients With Atherosclerotic Cardiovascular Disease. *JAMA Cardiol* 2019;**4**:206–213. doi: <https://doi.org/10.1001/jamacardio.2018.4936>
9. Kovanen PT, Bilheimer DW, Goldstein JL, Jaramillo JJ, Brown MS. Regulatory role for hepatic low density lipoprotein receptors in vivo in the dog. *Proc Natl Acad Sci U S A* 1981;**78**:1194–1198.
10. Lagace TA, Curtis DE, Garuti R, McNutt MC, Park SW, Prather HB, et al. Secreted PCSK9 decreases the number of LDL receptors in hepatocytes and in livers of parabiotic mice. *J Clin Invest* 2006;**116**:2995–3005. doi: <https://doi.org/10.1172/JCI29383>
11. Zhang D-W, Lagace TA, Garuti R, Zhao Z, McDonald M, Horton JD, et al. Binding of Proprotein Convertase Subtilisin/Kexin Type 9 to Epidermal Growth Factor-like Repeat A of Low Density Lipoprotein Receptor Decreases Receptor Recycling and Increases Degradation. *J Biol Chem* 2007;**282**:18602–18612. doi: <https://doi.org/10.1074/jbc.M702027200>
12. Brown M, Goldstein J. A receptor-mediated pathway for cholesterol homeostasis. *Science* 1986;**232**:34–47. doi: <https://doi.org/10.1126/science.3513311>
13. Islam MM, Hlushchenko I, Pfisterer SG. Low-Density Lipoprotein Internalization,

- Degradation and Receptor Recycling Along Membrane Contact Sites. *Front Cell Dev Biol* 2022;**10**.
14. Pfisterer SG, Brock I, Kanerva K, Hlushchenko I, Paavolainen L, Ripatti P, et al. Multiparametric platform for profiling lipid trafficking in human leukocytes. *Cell Rep Methods* 2022;**2**:100166. doi: <https://doi.org/10.1016/j.crmeth.2022.100166>
 15. Gaddi A, Arca M, Ciarrocchi A, Fazio S, D'Alò G, Tiozzo R, et al. Pravastatin in heterozygous familial hypercholesterolemia: Low-density lipoprotein (LDL) cholesterol-lowering effect and LDL receptor activity on skin fibroblasts. *Metabolism* 1991;**40**:1074–1078. doi: [https://doi.org/10.1016/0026-0495\(91\)90132-G](https://doi.org/10.1016/0026-0495(91)90132-G)
 16. Hagemenas FC, Illingworth DR. Cholesterol homeostasis in mononuclear leukocytes from patients with familial hypercholesterolemia treated with lovastatin. *Arterioscler Off J Am Heart Assoc Inc* 1989;**9**:355–361. doi: <https://doi.org/10.1161/01.ATV.9.3.355>
 17. Hagemenas FC, Pappu AS, Illingworth DR. The effects of simvastatin on plasma lipoproteins and cholesterol homeostasis in patients with heterozygous familial hypercholesterolaemia. *Eur J Clin Invest* 1990;**20**:150–157. doi: <https://doi.org/10.1111/j.1365-2362.1990.tb02262.x>
 18. Thedrez A, Blom DJ, Ramin-Mangata S, Blanchard V, Croyal M, Chemello K, et al. Homozygous Familial Hypercholesterolemia Patients With Identical Mutations Variably Express the LDLR (Low-Density Lipoprotein Receptor): Implications for the Efficacy of Evolocumab. *Arterioscler Thromb Vasc Biol* 2018;**38**:592–598. doi: <https://doi.org/10.1161/ATVBAHA.117.310217>
 19. Urdal P, Leren TP, Tonstad S, Lund PK, Ose L. Flow cytometric measurement of low density lipoprotein receptor activity validated by DNA analysis in diagnosing heterozygous familial hypercholesterolemia. *Cytometry* 1997;**30**:264–268.
 20. Raungaard B, Heath F, Brorholt-Petersen JU, Jensen HK, Faergeman O. Flow cytometric assessment of LDL receptor activity in peripheral blood mononuclear cells compared to gene mutation detection in diagnosis of heterozygous familial hypercholesterolemia. *Cytometry* 1999;**36**:52–59. doi: [https://doi.org/10.1002/\(sici\)1097-0320\(19990501\)36:1<52::aid-cyto7>3.0.co;2-1](https://doi.org/10.1002/(sici)1097-0320(19990501)36:1<52::aid-cyto7>3.0.co;2-1)
 21. Karlson BW, Palmer MK, Nicholls SJ, Lundman P, Barter PJ. Doses of rosuvastatin, atorvastatin and simvastatin that induce equal reductions in LDL-C and non-HDL-C: Results from the VOYAGER meta-analysis. *Eur J Prev Cardiol* 2016;**23**:744–747. doi: <https://doi.org/10.1177/2047487315598710>
 22. Adams SP, Sekhon SS, Wright JM. Rosuvastatin for lowering lipids. *Cochrane Database Syst Rev* John Wiley & Sons, Ltd; 2014; doi: <https://doi.org/10.1002/14651858.CD010254.pub2>
 23. Adams SP, Tsang M, Wright JM. Atorvastatin for lowering lipids. *Cochrane Database Syst Rev* John Wiley & Sons, Ltd; 2015; doi: <https://doi.org/10.1002/14651858.CD008226.pub3>
 24. Borodulin K, Tolonen H, Jousilahti P, Jula A, Juolevi A, Koskinen S, et al. Cohort Profile: The National FINRISK Study. *Int J Epidemiol* 2018;**47**:696–696i. doi: <https://doi.org/10.1093/ije/dyx239>
 25. Goldstein JL, Basu SK, Brown MS. [19] Receptor-mediated endocytosis of low-density lipoprotein in cultured cells. *Methods in Enzymology* Academic Press; 1983. p. 241–260. doi: [https://doi.org/10.1016/0076-6879\(83\)98152-1](https://doi.org/10.1016/0076-6879(83)98152-1)
 26. Reynolds GD, St. Clair RW. A comparative microscopic and biochemical study of the uptake of fluorescent and 125I-labeled lipoproteins by skin fibroblasts, smooth muscle cells, and peritoneal macrophages in culture. *Am J Pathol* 1985;**121**:200–211.
 27. Stephan Z, Yurachek E. Rapid fluorometric assay of LDL receptor activity by DiI-labeled LDL. *J Lipid Res* 1993;**34**:325–330. doi:

- [https://doi.org/10.1016/S0022-2275\(20\)40759-X](https://doi.org/10.1016/S0022-2275(20)40759-X)
28. Spandl J, White DJ, Peychl J, Thiele C. Live Cell Multicolor Imaging of Lipid Droplets with a New Dye, LD540. *Traffic* 2009;**10**:1579–1584. doi: <https://doi.org/10.1111/j.1600-0854.2009.00980.x>
 29. Stirling DR, Swain-Bowden MJ, Lucas AM, Carpenter AE, Cimini BA, Goodman A. CellProfiler 4: improvements in speed, utility and usability. *BMC Bioinformatics* 2021;**22**:433. doi: <https://doi.org/10.1186/s12859-021-04344-9>
 30. Chang C-L, Liou J. Phosphatidylinositol 4,5-Bisphosphate Homeostasis Regulated by Nir2 and Nir3 Proteins at Endoplasmic Reticulum-Plasma Membrane Junctions*. *J Biol Chem* 2015;**290**:14289–14301. doi: <https://doi.org/10.1074/jbc.M114.621375>
 31. Mars N, Lindbohm JV, Briotta Parolo P della, Widén E, Kaprio J, Palotie A, et al. Systematic comparison of family history and polygenic risk across 24 common diseases. *Am J Hum Genet* 2022;**109**:2152–2162. doi: <https://doi.org/10.1016/j.ajhg.2022.10.009>
 32. Ripatti P, Rämö JT, Mars NJ, Fu Y, Lin J, Söderlund S, et al. Polygenic Hyperlipidemias and Coronary Artery Disease Risk. *Circ Genomic Precis Med* 2020;**13**:e002725. doi: <https://doi.org/10.1161/CIRCGEN.119.002725>
 33. McKinney W. Data Structures for Statistical Computing in Python. Austin, Texas; 2010. p. 56–61. doi: <https://doi.org/10.25080/Majora-92bf1922-00a>
 34. Harris CR, Millman KJ, Walt SJ van der, Gommers R, Virtanen P, Cournapeau D, et al. Array programming with NumPy. *Nature* Nature Publishing Group; 2020;**585**:357–362. doi: <https://doi.org/10.1038/s41586-020-2649-2>
 35. Virtanen P, Gommers R, Oliphant TE, Haberland M, Reddy T, Cournapeau D, et al. SciPy 1.0: fundamental algorithms for scientific computing in Python. *Nat Methods* Nature Publishing Group; 2020;**17**:261–272. doi: <https://doi.org/10.1038/s41592-019-0686-2>
 36. Hunter JD. Matplotlib: A 2D Graphics Environment. *Comput Sci Eng* 2007;**9**:90–95. doi: <https://doi.org/10.1109/MCSE.2007.55>
 37. Pedregosa F, Varoquaux G, Gramfort A, Michel V, Thirion B, Grisel O, et al. Scikit-learn: Machine Learning in Python. *J Mach Learn Res* 2011;**12**:2825–2830.
 38. Waskom ML. seaborn: statistical data visualization. *J Open Source Softw* 2021;**6**:3021. doi: <https://doi.org/10.21105/joss.03021>
 39. Reiner Ž, Catapano AL, De Backer G, Graham I, Taskinen M-R, Wiklund O, et al. ESC/EAS Guidelines for the management of dyslipidaemias: The Task Force for the management of dyslipidaemias of the European Society of Cardiology (ESC) and the European Atherosclerosis Society (EAS). *Eur Heart J* 2011;**32**:1769–1818. doi: <https://doi.org/10.1093/eurheartj/ehr158>
 40. Nordestgaard BG, Tybjaerg-Hansen A. IDL, VLDL, chylomicrons and atherosclerosis. *Eur J Epidemiol* 1992;**8 Suppl 1**:92–98. doi: <https://doi.org/10.1007/BF00145358>
 41. Varbo A, Benn M, Tybjaerg-Hansen A, Jørgensen AB, Frikke-Schmidt R, Nordestgaard BG. Remnant cholesterol as a causal risk factor for ischemic heart disease. *J Am Coll Cardiol* 2013;**61**:427–436. doi: <https://doi.org/10.1016/j.jacc.2012.08.1026>
 42. Ruuth M, Nguyen SD, Vihervaara T, Hilvo M, Laajala TD, Kondadi PK, et al. Susceptibility of low-density lipoprotein particles to aggregate depends on particle lipidome, is modifiable, and associates with future cardiovascular deaths. *Eur Heart J* 2018;**39**:2562–2573. doi: <https://doi.org/10.1093/eurheartj/ehy319>
 43. Trinder M, Francis GA, Brunham LR. Association of Monogenic vs Polygenic Hypercholesterolemia With Risk of Atherosclerotic Cardiovascular Disease. *JAMA Cardiol* 2020;**5**:390–399. doi: <https://doi.org/10.1001/jamacardio.2019.5954>
 44. Khera AV, Won H-H, Peloso GM, Lawson KS, Bartz TM, Deng X, et al. Diagnostic Yield of Sequencing Familial Hypercholesterolemia Genes in Severe

Hypercholesterolemia. *J Am Coll Cardiol* 2016;**67**:2578–2589. doi:
<https://doi.org/10.1016/j.jacc.2016.03.520>

45. Powell EE, Kroon PA. Low density lipoprotein receptor and 3-hydroxy-3-methylglutaryl coenzyme A reductase gene expression in human mononuclear leukocytes is regulated coordinately and parallels gene expression in human liver. *J Clin Invest* 1994;**93**:2168–2174.

Legends

Table 1. Baseline characteristics of the analysed subject groups.

BMI, body mass index; LDL-C, low density lipoprotein cholesterol; Each of the statin groups are compared to the control group. * $p < 0.05$, ** $p < 0.01$, + $p < 0.001$.

Figure 1. Multiparametric readouts for cellular lipid storage and trafficking.

(A) Schematic presentation of fluorescent LDL uptake in cells and quantification as mean cell intensity (Int) and the number of LDL-filled organelles (No). (B) Quantification of cellular lipid storage by determining the number of lipid droplets (LD-No), the total cellular lipid droplet area (LD-Area) and the proportion of lipid droplet positive cells (LD-Pos). (C) Each of these readouts was measured in lipid-rich (R) condition (left) and lipid-poor (P) condition (right) in monocyte and lymphocyte populations. First, primary uptake readouts for lipid-rich and -poor conditions were combined into uptake scores (UPT-R and UPT-P) and lipid mobilisation score was calculated by combining the ratios of lipid storage parameters in lipid rich to lipid poor conditions. Then uptake and mobilisation scores were further combined into higher-order lipid trafficking (LT) scores (C).

Figure 2. Cellular scores are associated with blood lipid markers for statin recipients.

Both primary monocyte readouts such as LDL-filled organelle number in lipid-poor conditions (No-P) and combined lipid trafficking scores (LT) correlate negatively with circulating LDL cholesterol (A), total cholesterol (B) and Apolipoprotein(B) (C) in subjects on statin monotherapy. Minus sign represents control group (n=135) with no lipid-lowering medication use and plus sign represents subjects on statin monotherapy (n=133). The next three groups are for subjects receiving statin of moderate intensity and higher (>35%, n=60), subjects on high and very high intensity statin (>40%, n=39) and subjects on very high intensity statin therapy (>45%, n=30). * - $p < 0.05$, ** - $p < 0.01$.

Figure 3. Low lipid trafficking scores are associated with a pro-atherogenic lipoprotein profile for high-intensity statin recipients.

(A) Correlation heatmap of combined lipid trafficking (LT) score to different lipid concentrations in 14 lipoprotein subclasses in control subjects. PT stands for total particle concentration, CE – cholesterol ester concentration, CE % – percent of cholesterol ester in particles, TG – triglyceride concentration and TG % – percent of triglycerides in particles. Heatmap colours correspond to r_s range and are explained at the bottom left corner of the figure. (B) Correlation heatmap of LT score to 14 lipoprotein subclasses in high-intensity statin recipients '>40%' group. (C) Correlation heatmap of LT score to circulating concentration of different lipid species in control individuals versus high-intensity statin recipients '>40%' group. The species are as follows: total phosphoglycerides (Tot PG), phosphatidylcholine and other cholines (PC), sphingomyelins (SM), total cholines (TotCho), total fatty acids (Tot FA), 22:06 docosahexaenoic acid (DHA), 18:02 linoleic acid (LA), omega-3 and omega-6 fatty acids (FAW3 and FAW6), polyunsaturated fatty acids (PUFA), monounsaturated fatty acids (MUFA), saturated fatty acids (SFA), remnant cholesterol (Rem-C). (D) The lowest quintile of LT scores for high-intensity statin users shows a cholesterol ester profile which is similar to controls, whilst subjects within the highest quintile have significantly reduced CE concentrations. * - $p < 0.05$, ** - $p < 0.01$, + - $p < 0.001$

Figure 4. Cellular scores can be combined with LDL-PRS to improve the associations with LDL-c and other lipids.

(A) Cellular LDL uptake (UPT-P) correlates with LDL-PRS (inverted) in high-intensity statin users (>40%, n=39) but not in control subjects (CTRL, n=134). (B) Combining LDL-PRS (inverted) and LT score into one combined score improves associations to LDL-c concentration in control subjects (-, n=134), statin users (+, n= 131), and subject groups with increasing statin intensity (>35%, n=59), (>40%, n=39) and (>45%, n=30). (C)

Correlation heatmap of LDL-PRS (inverted) score to 14 lipoprotein subclasses in high-intensity statin recipients '>40%' group. PT stands for total particle concentration, CE – cholesteryl ester concentration (CE), CE % – percent of CE in particles, TG – triglyceride concentration and TG % - percent of TG in particles. Heatmap colors correspond to Spearman's rank range and are explained at the bottom right corner of the figure. (D)

Correlation heatmap of combined score of LDL-PRS with LT to 14 lipoprotein subclasses in high-intensity statin recipients '>40%' group. (E) Correlation heatmap of LDL-PRS (inverted) score and combined LDL-PRS-LT score to circulating concentration of different lipid species in high-intensity statin recipients '>40%' group. The species are as follows: total phosphoglycerides (Tot PG), phosphatidylcholine and other cholines (PC), sphingomyelins (SM), total cholines (TotCho), total fatty acids (Tot FA), 22:06 docosahexaenoic acid (DHA), 18:02 linoleic acid (LA), omega-3 and omega-6 fatty acids (FAW3 and FAW6), polyunsaturated fatty acids (PUFA), monounsaturated fatty acids (MUFA), saturated fatty acids (SFA), remnant cholesterol (Rem-C). * - $p < 0.05$, ** - $p < 0.01$, + - $p < 0.001$.

Figure 5. Using cellular scores to stratify subjects for LDL goal attainment.

(A) Percent of subjects achieving their LDL-C goals when being within the highest quintile of the LDL-PRS (green), lipid trafficking score (LT-R) (blue) or combined LDL-PRS/LT-R score (magenta) as compared to subjects without stratification (grey). (B) Odds ratios for achieving LDL-C target levels for subjects within the highest quintile of the LDL-PRS (green), LT-R(blue) and combined LDL-PRS/LT-R score for the same subject groups as in (A). (C) Percent of subjects achieving their target goals when being within the lowest quintile of the LDL-PRS (green), lipid trafficking score (LT-R) (blue) or combined LDL-PRS/LT-R score (magenta) as compared to subjects without stratification (grey). (D) Odds ratios for achieving LDL-C target levels for subjects within the lowest quintile of the LDL-PRS (green), LT-R (blue) and combined LDL-PRS/LT-R score for the same subject

groups as in (C). Control (-) group had 134 subjects and 27 in focus quintiles, statin group (-) had 131 subjects and 27 in focus quintiles, '>35%' group had 59 subjects and 12 in focus quintiles, '>40%' group consisted of 39 subjects and 8 per analysed quintile, '>45%' group has a total of 30 subjects with 6 in each quintile. Blue text in (B) and (C) indicates estimated odds ratios and confidence intervals. * - $p < 0.05$, ** - $p < 0.01$, + - $p < 0.001$.

Figure 6. Lipid mobilisation score in risk assessment for myocardial infarction and stroke.

Subjects in the lowest quintile of lipid mobilisation score have increased odds of experiencing a cardiovascular event as compared to the rest of the group. The odds ratio is higher with a concomitant increase in statin intensity. Control (-) group had 134 subjects (27 in focus quintile), statin group (-) had 131 subjects (27 in focus quintile), '>35%' group had 59 subjects (12 in focus quintile), '>40%' group consisted of 39 subjects (8 in focus quintile) and '>45%' group had a total of 30 subjects(6 in each quintile). * $p < 0.05$.

Table 1

	CONTROL (-)	STATIN (+)	>35%	>40%	>45%
Subject number	135	133	60	39	30
Sex, male, n (%)	69 (51%)	70 (53%)	33 (55%)	17 (44%)	14 (47%)
Mean (SEM):					
Age, years	62 (0.7)	63.2 (0.7)	63 (0.9)	64.2 (1.0)	64 (1.1)
BMI	27.8 (0.4)	28.6 (0.4)	28.5 (0.6)	28.9 (0.8)	29.7 (0.9)*
LDL-C, mmol/L	3.48 (0.07)	2.51 (0.07)+	2.41 (0.1)+	2.51 (0.14)+	2.52 (0.16)+
Total cholesterol, mmol/L	5.65 (0.08)	4.61 (0.08)+	4.52 (0.13)+	4.64 (0.18)+	4.64 (0.23)+
Triglycerides, mmol/L	1.5 (0.1)	1.54 (0.08)	1.6 (0.13)	1.7 (0.17)	1.74 (0.22)

Figure 1

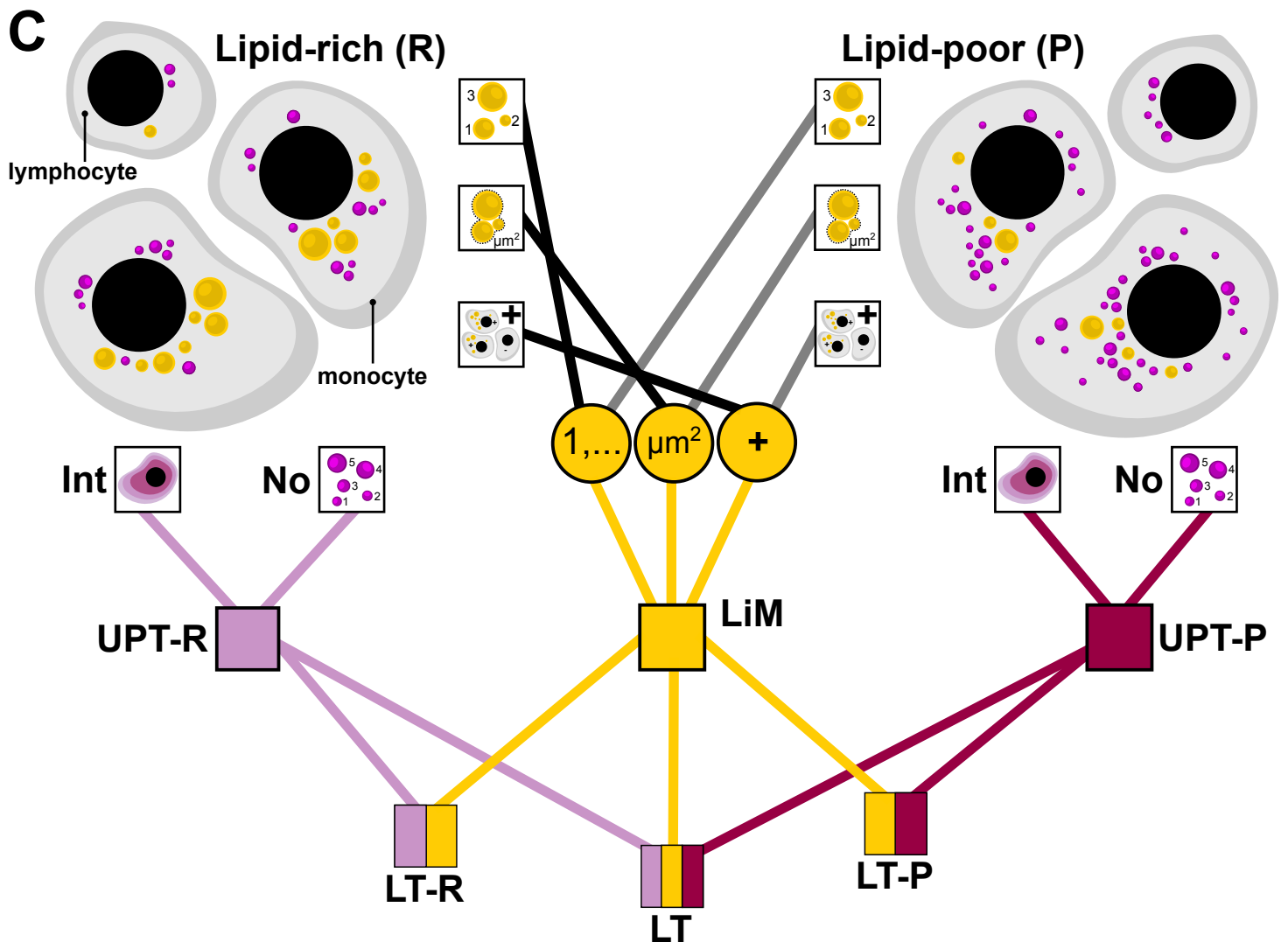
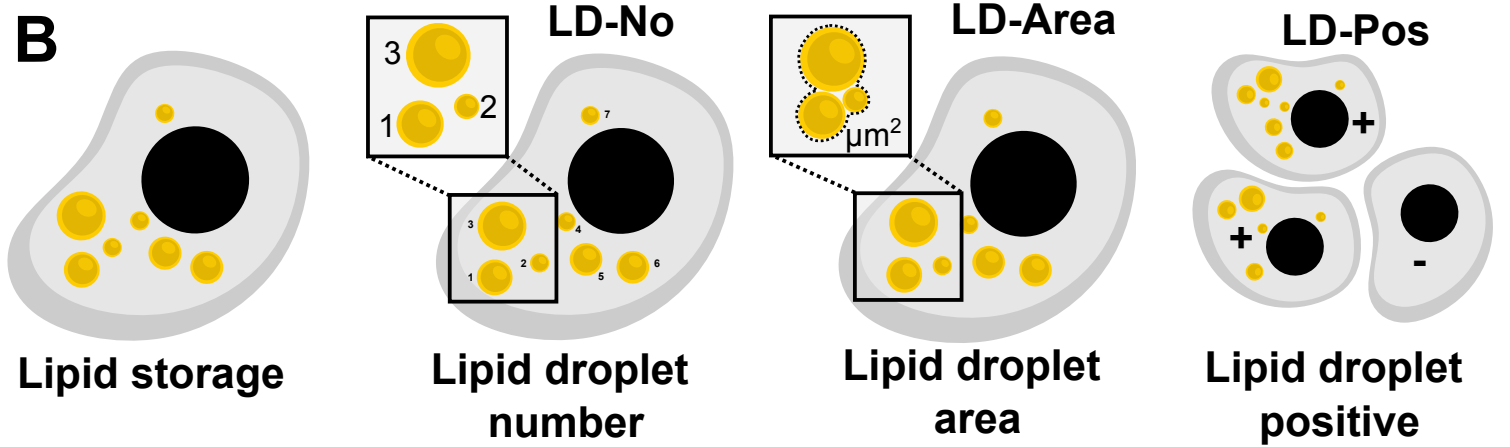
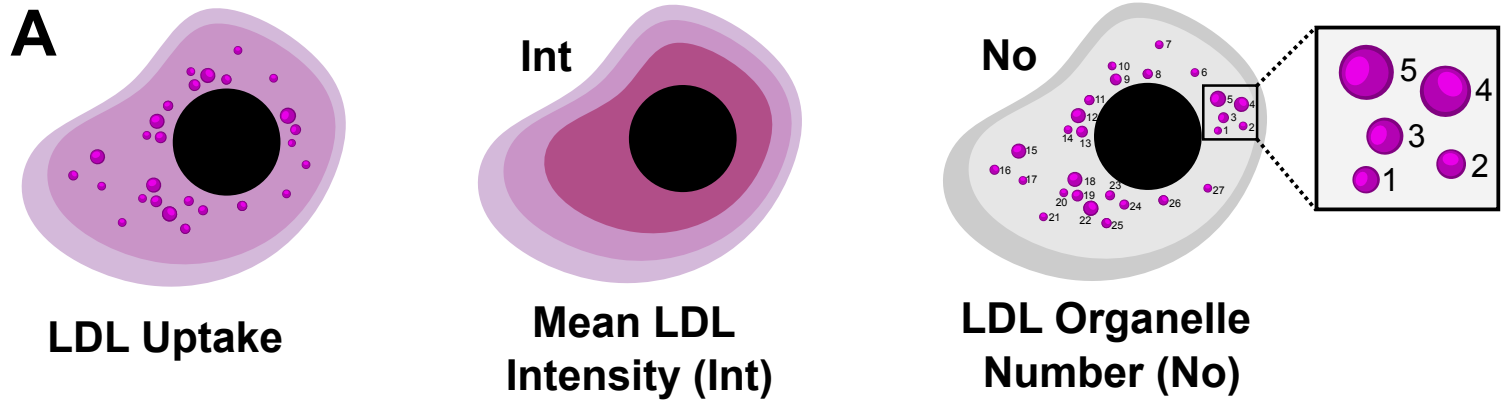


Figure 2

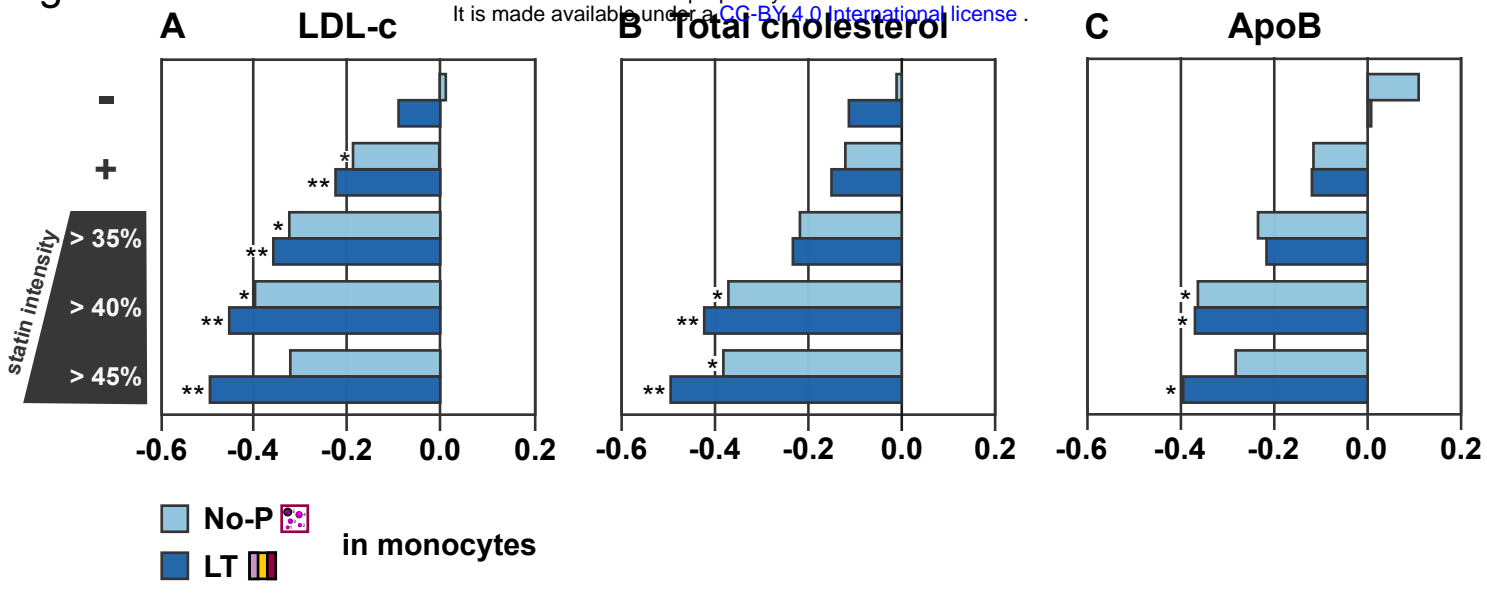


Figure 4

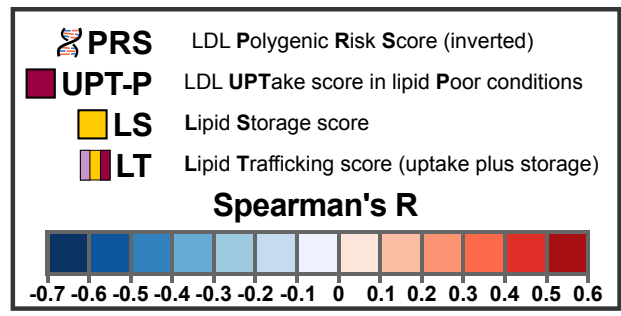
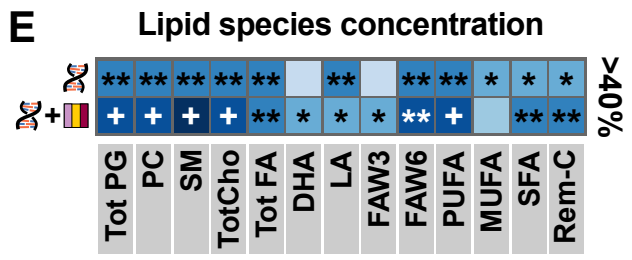
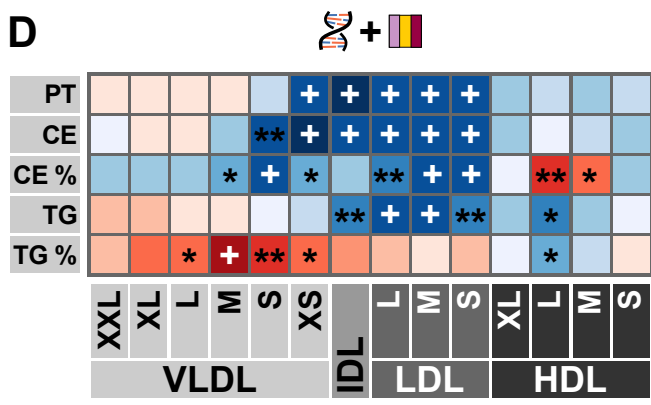
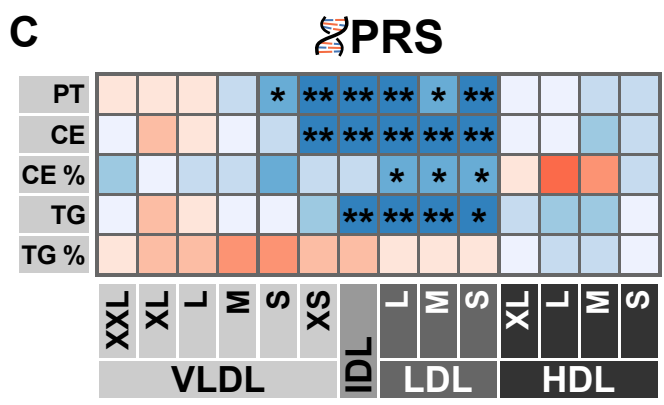
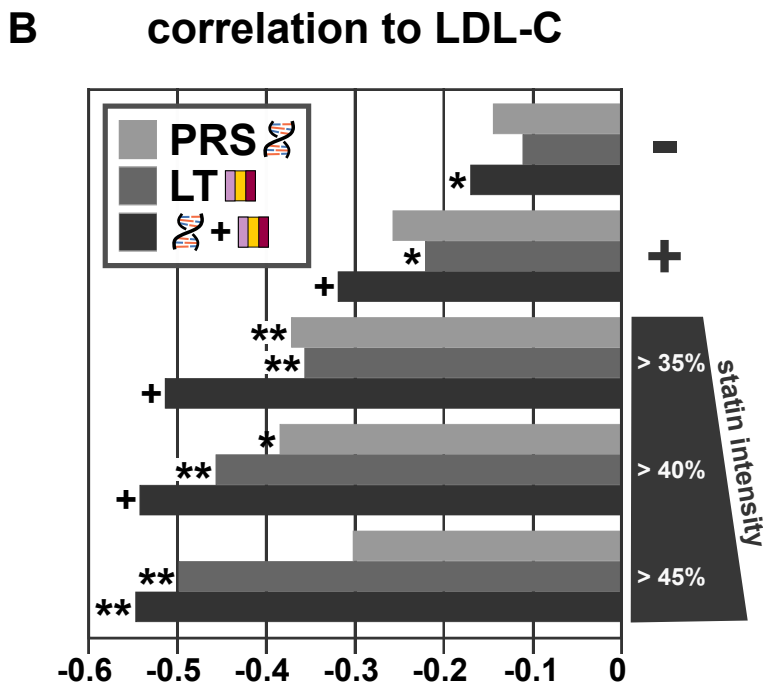
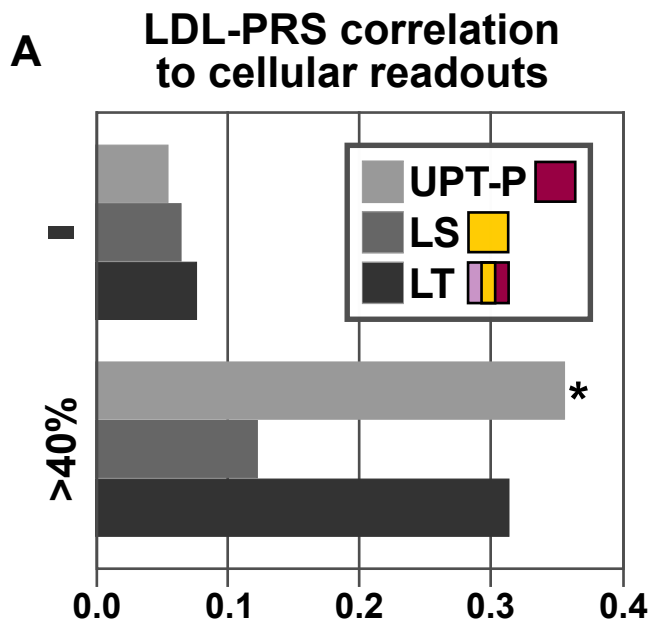


Figure 5

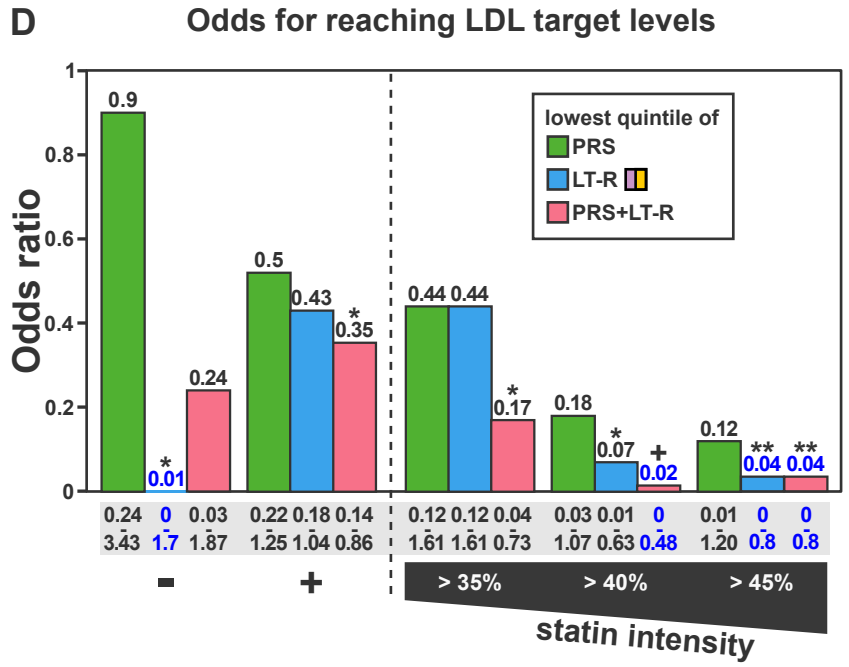
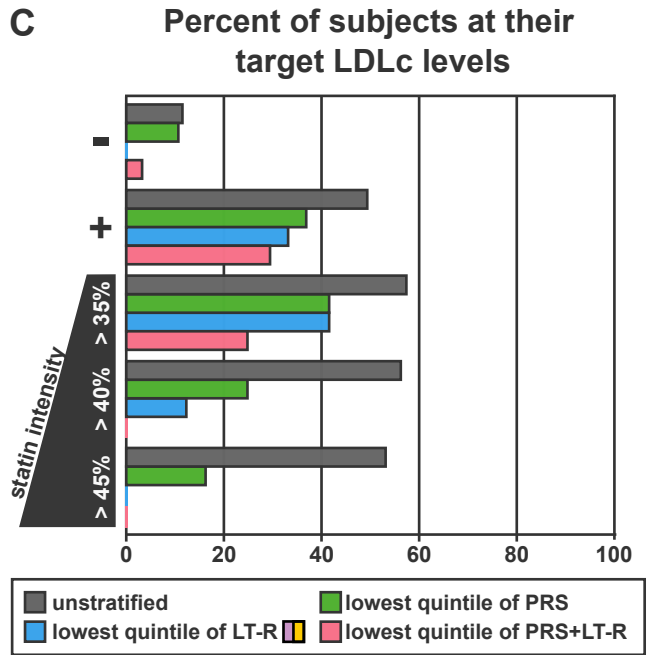
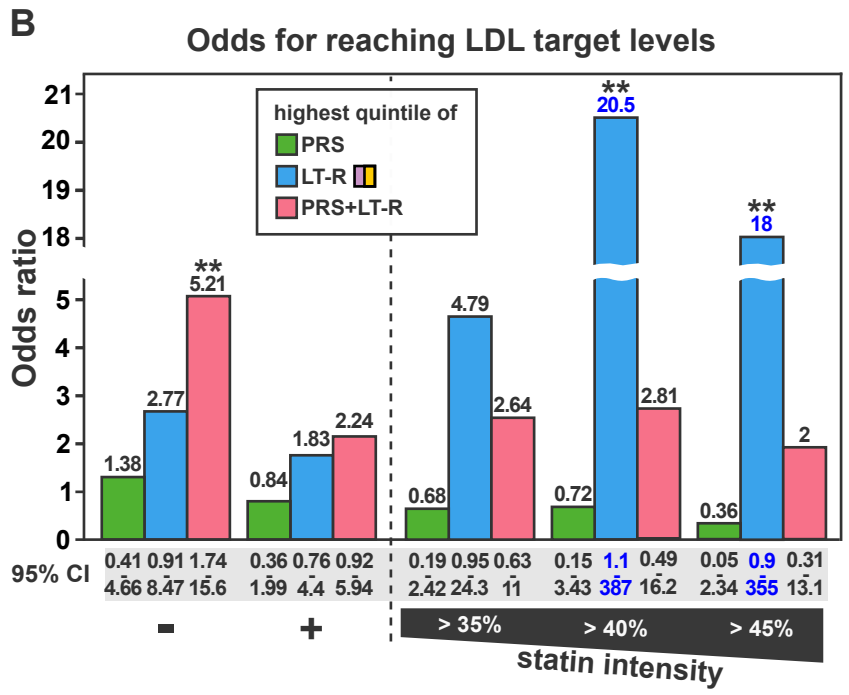
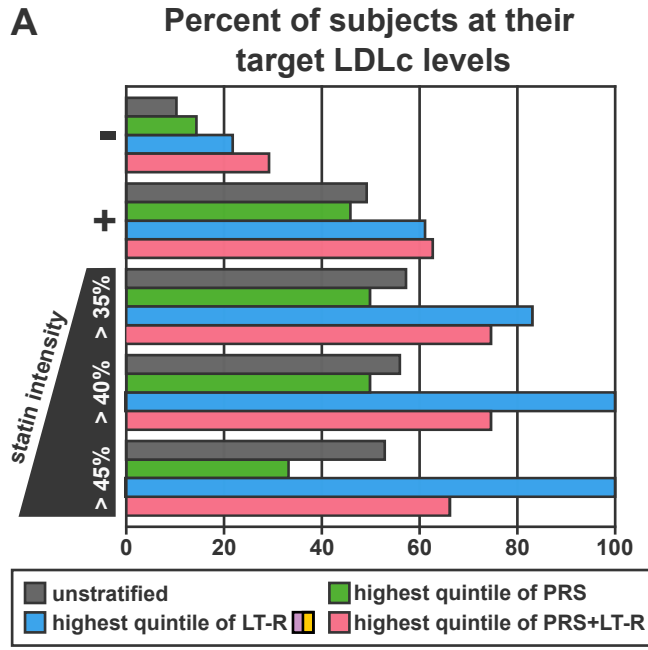
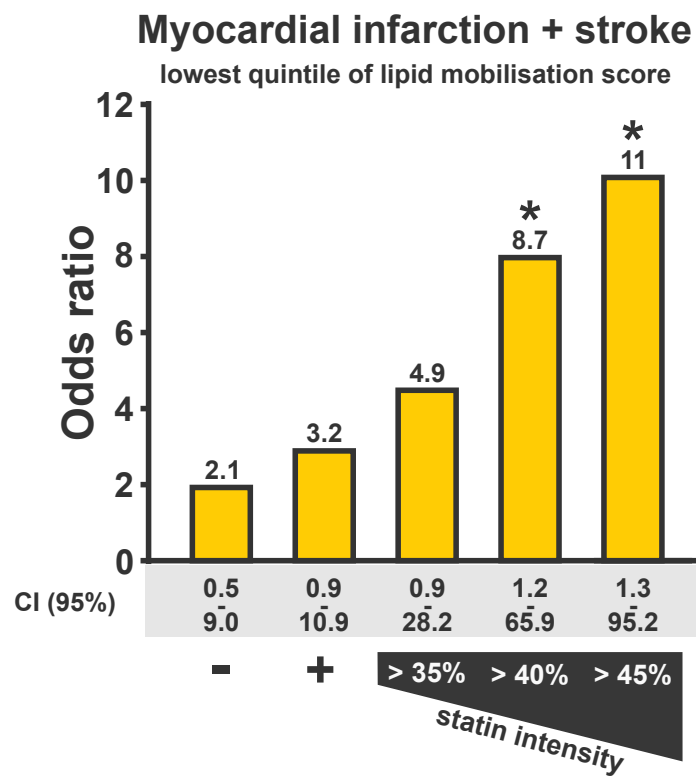


Figure 6



Graphical Abstract

